Shear work contribution to convective heat transfer of dilute gases in slip flow regime

SHEAR WORK CONTRIBUTION TO CONVECTIVE HEAT TRANSFER OF DILUTE GASES IN SLIP FLOW REGIME

Pamela Vocale[a*], Gian Luca Morini[b], Marco Spiga[a], Stéphane Colin[c]

[a]Department of Industrial Engineering, University of Parma, Parco Area delle Scienze 181/A, 43124 Parma, Italy

[b]DIN - Alma Mater Studiorum Università di Bologna, Viale Risorgimento 3, 40135 Bologna, Italy

[c]Université de Toulouse - Institut Clément Ader (ICA), 3 rue Caroline Aigle, 31400 Toulouse, France

*Corresponding author:

Pamela Vocale, Eng. Ph.D.

Phone: +39 0521 905855

Fax: +39 0521 905705

e-mail: pamela.vocale@unipr.it

ABSTRACT

In the literature some researchers highlighted that for a dilute gas in slip flow regime and in presence of a non negligible viscous heating, the analysis of the gas micro-convection has to be tackled by modifying the thermal boundary conditions to account for the shear work due to the slip at the wall. Although in the recent past a specific modified boundary condition has been proposed, theoretically justified and applied to investigate the effect of the shear work on the convective heat transfer in presence of dilute gases, in this paper is demonstrated that there is not a need of a modified boundary condition in order to take into account the effect of the shear work in the analysis of forced convection. In the present work by means of a comprehensive theoretical analysis is demonstrated that the modified boundary condition is useless for the analysis of the effect of shear work on the evaluation of the convective heat transfer coefficients in presence of a dilute gas with non-negligible viscous dissipation.

Moreover, to evaluate the inaccuracy of the results obtained by using the modified boundary conditions the difference, in terms of Nusselt number, between the exact and the approximate solution has been numerically estimated for elliptical microchannels. The numerical outcomes point out that the adoption of the modified boundary condition leads to an underestimation or an overestimation of the Nusselt numbers depending on the values of Brinkman number and on the channel cross section geometry.

KEYWORDS

Sliding friction; internal forced convection; dilute gas; viscous dissipation; microfluidics.

1. INTRODUCTION

When a gas flow is forced through a miniaturised heated channel, the effects due to the gas compressibility and rarefaction on convective heat transfer can be significant. For a fixed gas mass flow rate, the reduction of the inner channel dimensions increases the average velocity of the flow and the viscous dissipation tends to be coupled to the rarefaction and compressibility effects. The influence of these effects on the convective heat transfer coefficient has been investigated both theoretically and experimentally by many researchers in the last years, as highlighted by Kandlikar et al. [1] and by Colin [2] in their recent reviews.

In 1958 Maslen [3] highlighted how, in presence of a gas slip flow close to the solid wall of a channel, the calculation of the heat flux at the wall should include two contributions: one is the usual contribution due to the heat conduction at the wall and the second one is due to the sliding friction (i.e. the shear work due to the slip at the wall). However, the success met by the modified boundary condition proposed by Maslen has been scarce and in the succeeding technical papers devoted to the analysis of convective heat transfer of dilute gas flows in microchannels in slip flow regime, even in presence of significant viscous dissipation effects [4-8], the Nusselt numbers have been always calculated without accounting for the contribution due to the sliding friction at the wall. Only Sparrow and Lin [4] cited in their paper Maslen's boundary condition but the results presented in their paper were obtained by ignoring the conclusions of Maslen's paper. However, they observed how, in the case of uniform heat flux problem, the Nusselt numbers calculated in their paper by neglecting the effect of the shear work, result unchanged if the imposed wall heat flux is corrected by adding the contribution due to the shear work.

A renewed interest on Maslen's work was stimulated by the recent papers published by Hadjiconstantinou [9] and Hong and Asako [10]. Hadjiconstantinou [9] showed analytically that the shear work changes the total heat exchange at the wall for a dilute gas with negligible compressibility effects. He introduced two different Nusselt numbers in order to evaluate the thermal energy exchange and the total energy exchange between the wall and the dilute gas. Hong and Asako [10] tried to provide a theoretical justification to Maslen's boundary condition starting from the application of the energy balance equation for a gas flow through a circular channel and applying the gas kinetic theory. They concluded that in presence of slip flow and significant viscous dissipation effects the inclusion of the shear work contribution within the boundary condition, as proposed by Maslen, becomes mandatory and they explain in which way the boundary condition must be treated when the shear work is not negligible.

After the paper of Hong and Asako [10], Maslen's boundary condition has been applied by Myamoto [11] and by Ramadan and Tlili [12] who investigated convective heat transfer of dilute gases in parallel plates. These works demonstrated that, in presence of non-negligible viscous dissipation, the use of Maslen's boundary condition affects significantly the Nusselt number. The general conclusions of these works is that the usage of the modified boundary condition proposed by Maslen must be recommended for the determination of the convective heat transfer coefficient in the cases in which the viscous heating is significant. Another conclusion of these works is that the Nusselt numbers determined by the authors who ignored the Maslen's boundary condition (i.e. [4-8]) must be considered wrong.

Despite the huge work done in this field by many authors, it is opinion of the writers that it is still not clear when Maslen's boundary condition has to be applied in order to account for the contribution of the viscous dissipation on the convective heat transfer coefficient in presence of dilute gases in slip flow regime.

In order to clarify this issue, the present work provides a comprehensive theoretical analysis of the modelling of convective heat transfer in microducts aimed at explaining that no needs of a modified boundary condition exist for the analysis of convective heat transfer in presence of dilute gases with significant shear work. It will be demonstrated that the Maslen's boundary condition coupled to the energy equation is not able to give a good prediction of the exact Nusselt numbers in presence of dilute gases with significant viscous dissipation effects.

2. MATHEMATICAL MODEL

Let's consider a dilute gas flow through a microchannel having an axially uniform cross-section of area Ω and perimeter Γ (see Fig. 1). The following assumptions are made:

- all the transport processes are in a steady state,
- the gas is modelled as a Newtonian fluid in fully developed laminar regime,
- the gas density variation in the transverse direction are negligible,
- the gas properties are not dependent on the temperature,
- free convection, chemical reactions, electromagnetic effects and mass diffusion are neglected,
- channel walls are rigid, fixed and non-porous,
- the dilute gas flow is generated by a constant imposed axial pressure gradient dp/dz (pressure driven flow).

A Cartesian system of coordinates (x, y, z) is used with the z axis parallel to the axis of the channel. Under the previous hypotheses, the complete set of the governing balance equations for the analysis of forced convection of an ideal gas through the channel are the following:

$$\begin{aligned}
&\nabla \cdot \mathbf{v} = 0 \\
&\rho \frac{D\mathbf{v}}{Dt} = -\nabla p + (\nabla \cdot \boldsymbol{\tau}) \\
&\rho \frac{DH}{Dt} = -(\nabla \cdot q) + (\boldsymbol{\tau} : \nabla \mathbf{v}) + \frac{Dp}{Dt}
\end{aligned} \tag{1}$$

coupled with the constitutive laws for an ideal gas:

$$\rho = \frac{p}{RT}; \quad H = c_p T \tag{2}$$

where $\mathbf{v}$ indicates the velocity field, ρ the fluid density, t the time, p the pressure, $\boldsymbol{\tau}$ the stress tensor, H the gas enthalpy, q the heat flow, T the fluid temperature and c_p the specific heat at constant pressure.

Being in fully developed laminar regime, the velocity field has only axial component (u), which is independent of the channel axis (z), whereas the pressure field depends only on the axial coordinate.

Under the hypotheses summarized before the governing equations can be written as follows:

$$\begin{aligned}
&\frac{\partial u}{\partial z} = 0 \\
&-\rho u \frac{\partial u}{\partial z} = 0 = \frac{dp}{dz} - \mu \nabla^2 u \\
&\rho c_p u \frac{\partial T}{\partial z} = k \nabla^2 T + \mu (\nabla u \cdot \nabla u) + u \frac{dp}{dz}
\end{aligned} \tag{3}$$

where u is the gas local z-component of velocity, μ is the gas dynamic viscosity, $\partial T/\partial z$ is the axial component of the temperature gradient and k is the gas thermal conductivity.

In the energy balance equation, the first term of the r.h.s. is the diffusive heat flux, the second term represents the viscous dissipation term and the third term is the flow work. As highlighted by Shah and London [13], the flow work term appears when the energy and momentum balance equations are manipulated in order to eliminate the kinetic energy term.

By integrating the energy equation over the channel cross-section Ω one obtains:

$$\int_\Omega \rho c_p u \frac{\partial T}{\partial z} d\Omega = \int_\Omega k \nabla^2 T d\Omega + \mu \int_\Omega \nabla u \cdot \nabla u \, d\Omega + \int_\Omega u \frac{dp}{dz} d\Omega \tag{4}$$

It is possible to analyze separately each term of this equation; starting from the term on the l.h.s. of Eq.(4) and by considering a thermally fully developed H2 boundary condition (i.e. a uniform heat flux is imposed at the channel walls), one can write:

$$\frac{\partial T}{\partial z} = \frac{dT_b}{dz} \tag{5}$$

where T_b is the bulk temperature associated to the channel cross section.

It is possible to use Eq.(5) to write the term on the l.h.s. of Eq.(4) as follows:

$$\int_\Omega \rho c_p u \frac{\partial T}{\partial z} d\Omega = \rho c_p \frac{dT_b}{dz} \int_\Omega u d\Omega = \rho c_p W \Omega \frac{dT_b}{dz} \tag{6}$$

where W is the average velocity on the channel cross section of area equal to Ω.

By applying the divergence theorem to the first term of the r.h.s. of Eq.(4) one obtains:

$$\int_\Omega k \nabla^2 T d\Omega = k \int_\Omega (\nabla \cdot \nabla T) d\Omega = k \int_\Gamma (\nabla T \cdot (-\mathbf{n})) d\Gamma = \int_\Gamma q d\Gamma = q_{w,m} \Gamma \tag{7}$$

where $q_{w,m}$ is the average value of the imposed heat flux along the heated perimeter of the channel: in the case of a H2 boundary condition $q_{w,m}=q$.

The second term of the r.h.s. of Eq.(4) can be algebraically manipulated into:

$$\mu \int_\Omega \nabla u \cdot \nabla u \, d\Omega = \mu \left[\int_\Gamma (u \nabla u \cdot (-\mathbf{n})) d\Gamma - \int_\Omega (u \nabla^2 u) d\Omega \right] \tag{8}$$

The flow work term in Eq.(4) can be written in this form by using the momentum balance equation (Eq.(3)):

$$\int_\Omega u \frac{dp}{dz} d\Omega = \mu \int_\Omega (u \nabla^2 u) d\Omega \tag{9}$$

Using Eqs.(6),(7),(8) and (9) in Eq.(4) one obtains the following integral energy balance equation:

$$\rho c_p W \Omega \frac{dT_b}{dz} = q_{w,m} \Gamma + \mu \left[\int_\Gamma (u \nabla u \cdot (-\mathbf{n})) d\Gamma - \int_\Omega (u \nabla^2 u) d\Omega \right] + \mu \int_\Omega (u \nabla^2 u) d\Omega \tag{10}$$

Eq.(10) highlights that the increase in the bulk temperature along the channel axis is due to the heat flux imposed at the walls, to the viscous heating diminished by the cooling effect due to the flow work. If one is interested to calculate the algebraic sum of the heat generated by viscous dissipation and the cooling effect due to the flow work term, from Eq.(8) and (9) it is easy to demonstrate that:

$$\mu \Delta = \mu \int_\Omega (\nabla u \cdot \nabla u) d\Omega + \int_\Omega u \frac{dp}{dz} d\Omega = \mu \int_\Gamma (u \nabla u) \cdot (-\vec{n}) d\Gamma \tag{11}$$

Eq.(11) highlights that, if a no-slip velocity boundary condition is valid on the channel solid walls, Δ becomes identically zero. This means that for a perfect gas the heat generated by viscous dissipation on the whole cross-section is exactly balanced by the cooling effect due to the flow work term.

On the contrary, for a dilute gas in slip flow regime Δ is different from zero and assumes negative values; in this case Eq.(10) can be written as:

$$\rho c_p W \Omega \frac{dT_b}{dz} = q_{w,m}\Gamma + \mu\Delta \tag{12}$$

An alternative way to write Eq.(12) is the following:

$$\rho c_p W \Omega \frac{dT_b}{dz} = q^*_{w,m}\,\Gamma \tag{13}$$

where the "total energy flux at the wall" q^*_w is introduced:

$$q^*_{w,m} = q_{w,m} + \mu \frac{\int_\Gamma \left(u\nabla u\cdot(-\mathbf{n})\right) d\Gamma}{\Gamma} \tag{14}$$

Eq.(12) highlights that the bulk temperature increase along the axial direction is reduced by the combined effect due to both viscous dissipation and flow work in the case of a dilute gas (Δ<0). Eq.(14) puts in evidence that the combined effect due to viscous dissipation and flow work generates close to the solid wall a total energy exchange which is locally equal to:

$$q^*_{w,m} = -k\left.\frac{\partial T}{\partial n}\right|_w - \mu\left.\left(u\frac{\partial u}{\partial n}\right)\right|_w \tag{15}$$

Eq.(15) can be useful if the local total energy exchange between the gas and the wall must be determined, as done by Hadjiconstantinou [9]. Sparrow and Lin [4] suggested the use Eq.(15) as boundary condition in approximated forced convection mathematical models in which viscous dissipation and flow work are not accounted for in the energy equation.

It is a trivial conclusion that, in order to take into account the effect of the shear work on the Nusselt number, it is sufficient to consider within the energy balance equation both the viscous dissipation term and the flow work term without to modify the boundary condition (i.e. constant heat flux imposed at the wall). This point was not completely clarified by Hong and Asako in [10] where, after the derivation of the physical meaning of the shear work term, they suggest the inclusion of the shear work term in the boundary conditions used for the determination of the temperature distribution of dilute gases in slip regime

It is possible to conclude that the exact solution of the problem of the temperature field determination in the thermal fully developed region of a channel can be obtained, for H2 thermal boundary condition, by solving the momentum balance equation and by coupling the energy balance equation (Eq.(3)) with Eq.(12):

$$\begin{cases} \mu\nabla^2 u = \dfrac{dp}{dz} \\ \dfrac{u}{W\Omega}\left(q_{w,m}\Gamma + \mu\Delta\right) = k\nabla^2 T + \mu\left(\nabla u \cdot \nabla u\right) + u\dfrac{dp}{dz} \end{cases} \tag{16}$$

with the help of the usual thermal boundary condition for H2 problems:

$$-k\left.\frac{\partial T}{\partial n}\right|_w = q_{w,m} \tag{17}$$

and the first order slip-velocity and temperature jump boundary conditions at the walls:

$$\begin{cases} u_w - u_{wall} = \varpi_u \dfrac{2-\alpha}{\alpha}\lambda_{mfp}\left.\dfrac{\partial u}{\partial n}\right|_w \\ T_w - T_{wall} = \dfrac{2-\alpha_e}{\alpha_e}\dfrac{2\gamma}{\gamma+1}\dfrac{k}{\mu c_p}\lambda_{mfp}\left.\dfrac{\partial T}{\partial n}\right|_w \end{cases} \tag{18}$$

In Eq.(18) the momentum (α) and thermal (α_e) accommodation coefficients are invoked with γ, the specific heat ratio, and λ_{mfp}, the molecular mean free path. The coefficient ω_u is a corrective coefficient that must be added for a better prediction of the flow out of the Knudsen layer.

From the complete set of governing equations (Eq.(16-18)) for the description of forced convection of dilute gases in microchannels a series of different approximated models can be generated.

Here, three different cases are studied:

Case A (full model): In the complete energy balance equation (Eq.(16)) both flow work and viscous dissipation are accounted for, together with the classical H2 (Eq.(17)) and slip and jump boundary conditions (Eq.(18)).

This is the exact model suitable for the analysis of gas forced convection in microchannels.

Case B: Neglecting the flow work in the energy balance equation (Eq.(16)) with the modified boundary condition (Eq.(15)) coupled to slip and jump boundary conditions (Eq.(18)).

This approach has been followed by Ramadan and Tlili [12] for parallel plates.

Case C: Neglecting both flow work and viscous dissipation in the energy equation (Eq.(16)) but recovering their effect by means of the adoption of the modified boundary condition (Eq.(15)) coupled to slip and jump boundary conditions (Eq.(18)).

This approach, proposed in [4] and never used until now, represents a strong approximation of the complete model.

Now it becomes possible to compare the results obtained by solving the complete energy balance equation (Case A) with the results derived by the approximated models which use the modified boundary condition of Eq.(15) (Case B,C).

The complete expression of the differential problems linked to each model (from Case A to Case C), written in dimensionless form, is given in Appendix 1.

3. DISCUSSION OF THE RESULTS

With the aim of comparing the results, in terms of Nusselt numbers and temperature distributions, obtained by solving the three differential problems defined in Appendix 1 (Eqs.(A.8)-(A.12): Case A, B, C) Comsol Multiphysics® package has been used.

Following Hadjiconstantinou [10], two definitions of the Nusselt number can be introduced:

- the fully developed Nusselt number for H2 boundary condition based on the thermal energy exchange at the wall:

$$Nu = \frac{1}{\left(\bar{\theta}_w - \theta_b\right)} \tag{19}$$

being $\bar{\theta}_w$ the wall temperature averaged along the perimeter of the cross-section and θ_b the fluid bulk temperature.

- The fully developed Nusselt number based on the total energy exchange between wall and gas:

$$Nu_{sw} = \frac{1 - BrKnA_1 \left(\frac{\partial \overline{u}*}{\partial n*} \right)\Big|_w^2}{\left(\overline{\theta}_w - \theta_b\right)} \tag{20}$$

being $\left(\frac{\partial \overline{u}*}{\partial n*}\right)\Big|_w$ the velocity gradient at the wall and $\overline{\theta}_w$ the wall temperature both averaged along the perimeter of the cross-section.

In order to discuss the different results generated by adopting different models, microchannels featuring elliptical cross-sections with an aspect ratio β (defined as the ratio between the minor and the major axes) within the range 0.1 ÷ 1, have been considered. All the numerical results shown in this section have been obtained by adopting a first order slip velocity boundary condition (A_1=1) and a first order jump temperature boundary condition (B_1=1.6667).

The numerical procedure has been validated resorting to numerical data and/or analytical solutions available in literature for circular microchannels. The mesh independence analysis has been carried out by adopting six grid sizes for each value of the aspect ratio, Knudsen number and Brinkman number considered in the present analysis. The discretization error has been estimated by applying the Richardson extrapolation method [14-15]. In Table 1 the values of the Nusselt number calculated by using Eq.(19) for case A as a function of the adopted meshes are shown as a function of the elliptical aspect ratio (β = 1 and β = 0.1) and of the Knudsen number for a Brinkman number equal to 0.1. The relative difference ε_r between the Nusselt number obtained for a fixed grid size with respect to the Nusselt number obtained by adopting the finest mesh is reported in Table 1. From the results quoted in Table 1 it is evident that the shallow elliptical cross sections (lower β values) need a number of finite elements larger than the circular geometry (β=1) in order to reach the independence of the Nusselt number from the grid size. In this analysis the adopted meshes are characterized by a number of finite elements ranging between 3325 for β=1 and 25592 for β = 0.1.

The Nusselt numbers (Eq.(19)) calculated by solving numerically case A have been compared with the analytical values obtained by Aydin and Avci [8] for a circular channel β=1 as a function of the Knudsen number for Br = 0.1 (Figure 2a) and Br = -0.1 (Figure 2b). Figure 2 shows that a very good agreement in terms of Nusselt numbers obtained by solving case A and the values obtained by Aydin and Avci [8] there exists.

The good agreement shown by Fig. 2 with the analytical Nusselt numbers obtained for circular channels by Aydin and Avci [8] can be considered a benchmark for the numerical solution adopted in this paper. As additional comparison, the Nusselt numbers based on the thermal energy exchange (Eq.(19)) obtained by Hooman [16] for Br=0.01 and Br=0.001 and 0<Kn<0.1 have been used as comparison for the results obtained solving case A; also in this case the agreement is very good.

In Figure 3 a comparison between the Nusselt number based on the thermal energy exchange at the wall (Nu, Eq.(19)) and the Nusselt based on the total energy exchange between gas and wall (Nu_{sw}, Eq.(20)) is shown by considering case A for an elliptical microchannel with β=0.5 (Fig. 3a) and β=0.1 (Fig. 3b). The Nusselt number based on Eq.(19) (Nu) is always larger than the one based on Eq.(20) (Nu_{sw}) and, as expected, the difference between Nu and Nu_{sw} increases when the Brinkman number increases. The effect of the Brinkman number on Nu is weak in shallow elliptical channels (β=0.1); on the contrary, for increasing Br between 0.02 and 0.1 Nu_{sw} is significantly reduced. It is evident that for shallow elliptical channels the variation of both Nu and Nu_{sw} with Kn is small. The difference existing between Nu and Nu_{sw} (Fig. 3) highlights that the effect of the shear work on the total energy exchange between gas and walls is significant also for large Knudsen numbers when Br>0.02. This means that in the energy equation the viscous dissipation term and the flow work terms have to be considered if an accurate evaluation of the total energy exchange is needed.

In Fig. 4 the comparison between the Nusselt number (Nu) based on the thermal energy exchange (Eq.(19)) obtained by adopting the complete model (case A) and the other models described before (case B, C) in which the modified boundary condition (Eq.(15)) is used) is shown for a circular channel (β = 1).

It is evident that the models which use the modified boundary condition (case B and C) tend to overestimate the Nusselt number for positive Brinkman numbers (heated channels, Fig. 4a) and to underestimate the Nusselt number for negative Brinkman numbers (cooled channels, Fig. 4b).

This result highlights that the adoption of the modified boundary condition (Eq.(15)), used in the case B and C, is never able to recover the exact results in terms of Nusselt numbers in the range of Knudsen numbers considered here (Kn<0.1) when Br goes from -0.1 to 0.1. The maximum difference between the exact Nusselt number and the Nusselt number obtained by using the modified boundary condition (case B, C) is equal to 11.55% for Kn=0.06 (case B) and 38.28% for Kn=0.02 (case C).

In Figure 5 the trend of Nu_{sw} based on the total energy exchange between gas and channel walls is shown as a function of Knudsen number for Br=0.1 (Fig. 5a) and Br=-0.1 (Fig. 5b). It is evident that case B and C tend to overestimate or underestimate the value of Nu_{sw} in the whole range of Knudsen numbers considered here (Kn<0.1). The maximum difference between the exact Nu_{sw} and the Nu_{sw} obtained by using the modified boundary condition (case B, C) is equal to 11.49% for Kn=0.06 (case B) and 38.26% for Kn=0.02 (case C). These results highlight that similar results are obtained by working with Nu and Nu_{sw}.

Now, attention is focused on the values assumed by the Nusselt number based on the thermal energy exchange at the wall (Nu) because this parameter has been obtained by many authors by means of different models [4,5,6,8,12].

The influence of the channel geometry has been investigated by considering other values of the aspect ratio of the elliptical cross-section, namely β = 0.5 and β = 0.1. The comparison between the different approaches (from case A to case C), in terms of Nusselt numbers based on the thermal energy exchange at the wall (Eq.(19)), is shown in Figure 6 and in Figure 7 for β = 0.5 and β = 0.1, respectively, as a function of Knudsen number (Kn<0.1) keeping Br = 0.1 and Br = -0.1.

The numerical outcomes shown in Figure 6 and 7 point out that the discrepancy between the results of the exact solution (case A) and of the approximate solutions (case B, C) increases as the value of the aspect ratio increases and for large values of Br. It is also evident that for shallow elliptical channels (β = 0.1) the Nusselt numbers numbers based on the thermal energy exchange at the wall (Eq.(19)) is weakly dependent on the Knudsen number for a fixed value of Brinkman. On the contrary, the Nusselt numbers obtained by case B and C tend to be overestimated for positive values of Br and underestimated for negative Br; the maximum difference between the Nusselt numbers calculated by using case B and C and the exact Nusselt number tends to increase when Kn increases for a fixed value of Br; its value is about 25% for Kn=0.1 and Br=0.1 and -21% for Kn=0.1 and Br=-0.1. These values confirm that the modified boundary condition (Eq.(15)) is not able to give right values of Nu in presence of significant viscous dissipation and gas rarefaction also for shallow elliptical channels.

In Table 2 the maximum deviation (in percentage) from the exact value of Nu and Nu_{sw} is given for case B and C as a function of the channel aspect ratio. The values shown in Table 2 underline that the maximum inaccuracy in terms of Nu and Nu_{sw} obtained for case B and C ranges between ±10% and ±40%. Since the adoption of the modified boundary condition (Eq.(15)) is not theoretically based, as demonstrated in the previous section of this paper, and the computational effort linked to the solution of the complete equation set (case A) and of the simplified models in which the modified boundary condition is used (case B, C) is almost the same, the results shown in this paper suggest to avoid the use of approximated approaches in order to study forced convection in presence of dilute gas flows when the viscous heating cannot be disregarded.

4. CONCLUSIONS

In this paper a theoretical analysis of convective heat transfer in microducts has been carried out in order to clarify the role played by the viscous dissipation term and by the flow work term in the energy balance of a dilute gas flow in slip flow regime. The study was focused on the analysis of the contribution due to the sliding friction (i.e. the shear work due to the slip at the wall) on the total energy exchange between gas and wall with the aim of explaining if the adoption of a modified thermal boundary condition which accounts for this contribution can be useful for the estimation of the Nusselt number. The analysis reveals that, in order to take into account the effect due to the shear work, no modified boundary conditions at the walls are needed. To evaluate the inaccuracy of the results obtained by adopting models in which the modified boundary condition is used, the difference, in terms of Nusselt number, between the exact and the approximate solution has been numerically estimated for elliptical microchannels. The numerical outcomes point out that the discrepancy between the exact and approximate solution is significantly affected by Knudsen and Brinkman numbers and by the geometry of the channel cross-section; in general, the adoption of the modified boundary condition (Eq.(15)) is able to give Nusselt numbers underestimated for negative values of Br and overestimated in case of positive Br. The difference between the approximated Nusselt numbers and the exact ones increases for elliptical channels having a large aspect ratio; the difference tends to reach its maximum value for large Knudsen numbers in shallow elliptical microchannels ($\beta<0.5$) and at low Knudsen numbers for $\beta \geq 0.5$.

APPENDIX 1

In this appendix the governing equations for the analysis of forced convection for a dilute gas through a microchannel are written in dimensionless form by considering the following rules:

- all spatial quantities, except the axial coordinate z, are scaled with the hydraulic diameter (i.e. $D_h = 4\dfrac{\Omega}{\Gamma}$):

$$x^* = \frac{x}{D_h} \quad ; \quad y^* = \frac{y}{D_h} \quad ; \quad z^* = \frac{z}{D_h\, Re\, Pr} = \frac{z}{D_h\, Pe} \;;\; \nabla^* = D_h \nabla \;;\; \mathrm{Re} = \frac{\rho W D_h}{\mu} \;;\; Pe = Pr\ Re \tag{A.1}$$

- the velocity u is scaled with the average fluid velocity W;
- the temperature is scaled as follows:

$$\theta = k\frac{\left(T - T_0\right)}{q_{w,m} D_h} \tag{A.2}$$

In addition, it is useful to introduce further dimensionless quantities:

- the dimensionless pressure gradient (p^*), linked to the Poiseuille number (fRe, defined as the product between the Fanning friction factor f and the Reynolds number Re):

$$p^* = 2\,fRe = -\frac{D_h^2}{\mu W}\frac{dp}{dz} \tag{A.3}$$

- the Brinkman number (Br), which represents the ratio between the heat produced by viscous dissipation and the heat transferred by conduction, is invoked to account for viscous dissipation:

$$Br = \frac{\mu W^2}{q_{w,m} D_h} \tag{A.4}$$

- the Knudsen number (Kn), defined as the ratio of the mean free molecular path of the gas (λ_{mfp}) to the hydraulic diameter of the channel, is introduced to represent the gas rarefaction degree:

$$Kn = \frac{\lambda_{mfp}}{D_h} \tag{A.5}$$

By using these rules and the main dimensionless quantities introduced before, the momentum balance equation can be written in dimensionless form together with the first order slip boundary condition [2] as follows:

$$\begin{aligned} &\nabla^{*2} u^* + p^* = 0 \\ &u^*\big|_w = A_1 Kn \frac{\partial u^*}{\partial n^*}\bigg|_w \end{aligned} \tag{A.6}$$

being A_1 a coefficient linked to the momentum accommodation factor between the solid wall and the dilute gas (α) and the coefficient ϖ_u recalled in Eq.(18).

$$A_1 = \varpi_u \frac{2-\alpha}{\alpha} \tag{A.7}$$

In a pure forced convection problem the velocity calculation can be uncoupled by the temperature calculation. If the velocity field is obtained by solving Eq.(A.6) one can determine the temperature field by solving the following differential problems written in dimensionless form:

- Case A (full solution):

$$\begin{cases} 4u^*\left(1 + \dfrac{Br\Delta^*}{\Gamma^*}\right) = \nabla^{*2}\theta + Br\left[\nabla^* u^* \cdot \nabla^* u^* - p^* u^*\right] \\ \dfrac{\partial \theta}{\partial n^*}\bigg|_w = -1 \\ \theta\big|_w = B_1 Kn \dfrac{\partial \theta}{\partial n^*}\bigg|_w = -B_1 Kn \end{cases} \tag{A.8}$$

where B_1 is a coefficient linked to the thermal accommodation factor between the solid wall and the dilute gas (α_e), the Prandtl number and the specific heat ratio γ recalled in Eq.(18).

$$B_1 = \frac{2-\alpha_e}{\alpha_e}\frac{2\gamma}{\gamma+1}\frac{1}{\Pr} \tag{A.9}$$

In the energy equation Δ^* appears which depends on the dimensionless velocity profile and the microchannel cross-section only:

$$\Delta^* = \int_{\Gamma^*} \left(u^* \nabla^* u^* \cdot (-\mathbf{n})\right) d\Gamma^* \tag{A.10}$$

- Case B (flow work neglected and the modified boundary condition):

$$\begin{cases} 4u^*\left(1+\dfrac{Br\Phi^*}{\Gamma^*}\right)=\nabla^{*2}\theta+Br\left[\nabla^* u^*\cdot\nabla^* u^*\right] \\ \left.\dfrac{\partial\theta}{\partial n^*}\right|_w=-1+Br\left.\left(u^*\dfrac{\partial u^*}{\partial n^*}\right)\right|_w=-1+A_1 BrKn\left.\left(\dfrac{\partial u^*}{\partial n^*}\right)^2\right|_w \\ \theta|_w=B_1 Kn\left.\dfrac{\partial\theta}{\partial n^*}\right|_w \end{cases} \tag{A.11}$$

- Case C (flow work and viscous dissipation neglected and the modified boundary condition):

$$\begin{cases} 4u^*=\nabla^{*2}\theta \\ \left.\dfrac{\partial\theta}{\partial n^*}\right|_w=-1+Br\left.\left(u^*\dfrac{\partial u^*}{\partial n^*}\right)\right|_w=-1+A_1 BrKn\left.\left(\dfrac{\partial u^*}{\partial n^*}\right)^2\right|_w \\ \theta|_w=B_1 Kn\left.\dfrac{\partial\theta}{\partial n^*}\right|_w \end{cases} \tag{A.12}$$

NOMENCLATURE

A_1	First order coefficient of the slip boundary condition
B_1	First order coefficient of the temperature jump boundary condition
Br	Brinkman number
c_p	Specific heat at constant pressure
D_h	Hydraulic diameter of the channel
f	Fanning friction factor
h	Convective heat transfer coefficient
H	Gas enthalpy
k	Fluid thermal conductivity
Kn	Knudsen number, $\lambda_{\mathrm{mfp}} / D_h$
n	Normal coordinate at the internal walls of the cross-section
n^*	Dimensionless normal coordinate at the internal walls of the cross-section
Nu	Nusselt number, hD_h/k
p	Fluid pressure
p^*	Dimensionless fluid pressure
Pe	Péclet number
Pr	Prandtl number
Re	Reynolds number
q	Heat flux
t	Time
T	Fluid temperature
u	z-component of velocity
u^*	Dimensionless z-component of velocity
v	Velocity field
W	Average fluid velocity
x,y,z	Dimensionless Cartesian coordinates
x^*,y^*,z^*	Dimensionless Cartesian coordinates

Greek symbols

α	Momentum accommodation coefficient
α_e	Thermal accommodation coefficient
β	Aspect ratio

Γ	Perimeter of the cross-section
Γ^*	Dimensionless perimeter of the cross-section
θ	Dimensionless fluid temperature
λ_{mfp}	Mean free path of the fluid particles
μ	Fluid dynamic viscosity
ρ	Fluid density
τ	Stress tensor
ω	Corrective coefficient appeared in Eq.(18)
Ω	Cross-section area
Ω^*	Dimensionless cross-section area

Subscripts

b	Bulk
w	Wall

REFERENCES

[1] S.G. Kandlikar, S. Colin, Y. Peles, S. Garimella, R.F. Pease, J.J. Brandner, Heat Transfer in Microchannels - 2012 Status and Research Needs, Journal of Heat Transfer 135 (2013) 091001.

[2] S. Colin, Gas Microflows in the Slip Flow Regime: A Critical Review on Convective Heat Transfer, Journal of Heat Transfer 134 (2012) 020908.

[3] S.H. Maslen, On Heat Transfer in Slip Flow, Journal of the Aerospace Sciences 25 (6) (1958) 400-401.

[4] E.M. Sparrow, S.H. Lin, Laminar Heat Transfer in Tubes Under Slip-Flow Conditions, Journal of Heat Transfer 84 (1962) 363-369.

[5] G. Tunc, Y. Bayazitoglu, Heat transfer in microtubes with viscous dissipation, International Journal of Heat and Mass Transfer 44 (2001) 2395-2403.

[6] L. Kuddusi, E. Çetegen, Prediction of temperature distribution and Nusselt number in rectangular microchannels at wall slip condition for all versions of constant heat flux, Int. J. Heat Fluid Flow 28 (2007) 777–786.

[7] J. van Rij, T. Ameel, T. Harman, An evaluation of secondary effects on microchannel frictional and convective heat transfer characteristics, International Journal of Heat and Mass Transfer 52 (2009) 2792-2801.

[8] O. Aydın, M. Avcı, Heat and fluid flow characteristics of gases in micropipes, International Journal of Heat and Mass Transfer 49 (2006) 1723-1730.

[9] N.G. Hadjiconstantinou, Dissipation in Small Scale Gaseous Flows, ASME J. Heat Transfer, 125 (2003) 944-997.

[10] C. Hong, Y. Asako, Some considerations on thermal boundary condition of slip flow, International Journal of Heat and Mass Transfer 53 (2010) 3075-3079.

[11] M. Myamoto, W. Shi, Y. Katoh, J. Kurima, Choked flow and heat transfer of low density gas in a narrow parallel-plate channel with uniformly heating walls, International Journal of Heat and Mass Transfer 46 (2003) 2685-2693.

[12] K. Ramadan, I. Tlili, A Numerical Study of the Extended Graetz Problem in a Microchannel with Constant Wall Heat Flux: Shear Work Effects on Heat Transfer, Journal of Mechanics 31 (2015) 733-743.

[13] R.K. Shah, A.L. London, Laminar Flow Forced Convection in Ducts, Academic Press, New York, 1978.

[14] L.F. Richardson, J.A. Gaunt, The Deferred Approach to the Limit, Philos. Trans. R. Soc. London, Ser. A 226 (1927) 229-361.

[15] S.A. Richards, Completed Richardson extrapolation in space and time, Communications in Numerical Methods in Engineering, 13 (1997) 573-582.

[16] K. Hooman, Entropy Generation for Microscale Forced Convection: Effects of Different Thermal Boundary Conditions, Velocity Slip, Temperature Jump, Viscous Dissipation, and Duct Geometry, International Communications in Heat and Mass Transfer, 34 (2007) 945–957.

Figure captions

Figure 1 – Sketch of a straight microchannel with constant cross section and Cartesian coordinate system.

Figure 2 – Comparison between the Nusselt numbers obtained as a function of the Knudsen number by solving numerically case A (A_I=1, B_I=1.6667) and the analytical values reported in [8] for $\beta = 1$ and: (a) Br = 0.1 (b) Br = -0.1

Figure 3 – Comparison between the Nusselt number based on the thermal energy exchange at the wall (Nu, Eq.(19), continuous line) and the Nusselt number based on the total energy exchange between gas and wall (Nu_{sw}, Eq.(20), dashed line) as a function of the Knudsen number for fixed values of Br(Br=0.02, ○; Br=0.06, □; Br=0.1, ◇).Calculations made with model A (A_I=1, B_I=1.6667) for (a) $\beta = 0.5$ and (b) $\beta = 0.1$.

Figure 4 – Comparison between the Nusselt numbers based on the thermal energy exchange at the wall (Nu, Eq.(19)) obtained by the different models (A, B, C) as a function of the Knudsen number for a circular channel (β=1) ($\alpha = 1$, $\omega_u = 1$, $\alpha_e = 1$, $\gamma = 1.4$, $Pr = 0.7$) and: (a) Br = 0.1 (b) Br = -0.1.

Figure 5 – Comparison between the Nusselt numbers based on the total energy exchange at the wall (Nu_{sw}, Eq.(20)) obtained by the different models (A, B, C) as a function of the Knudsen number for an elliptical channel (β=1) ($\alpha = 1$, $\omega_u = 1$, $\alpha_e = 1$, $\gamma = 1.4$, $Pr = 0.7$) and: (a) Br = 0.1 (b) Br = -0.1.

Figure 6 – Comparison between the Nusselt numbers based on the thermal energy exchange at the wall (Nu, Eq.(19)) obtained by the different models (A, B, C) as a function of the Knudsen number for an elliptical channel (β=0.5) ($\alpha = 1$, $\omega_u = 1$, $\alpha_e = 1$, $\gamma = 1.4$, $Pr = 0.7$) and: (a) Br = 0.1 (b) Br = -0.1.

Figure 7 –Comparison between the Nusselt numbers based on the thermal energy exchange at the wall (Nu, Eq.(19)) obtained by the different models (A, B, C) as a function of the Knudsen number for a shallow elliptical channel (β=0.1) ($\alpha = 1$, $\omega_u = 1$, $\alpha_e = 1$, $\gamma = 1.4$, $Pr = 0.7$) and: (a) Br = 0.1 (b) Br = -0.1.

Table captions

Table 1 – Mesh sensitivity of the Nusselt number by varying the Knudsen number from 0 to 0.1 for a circular (β =1) and a shallow elliptical channel (β = 0.1) and for Br = 0.1.

Table 2 – Maximum deviation from the exact value of Nu and Nu_{sw} by using models involving the modified boundary condition (Eq.(15)) (case B and C) as a function of the channel aspect ratio β for elliptical microchannels.

Table 1.

β =1	Adopted (3325)	Mesh #1 (252)		Mesh #2 (364)		Mesh #3 (544)		Mesh #4 (938)		Mesh #5 (1922)	
Kn	Nu	Nu	ε_r	Nu	ε_r	Nu	ε_r	Nu	ε_r	Nu	ε_r
0	3.0380	3.0381	0.004%	3.0380	0.002%	3.0380	0.001%	3.0380	0.000%	3.0380	0.000%
0.02	3.2086	3.2087	0.003%	3.2086	0.001%	3.2086	0.001%	3.2086	0.000%	3.2086	0.000%
0.04	3.1937	3.1938	0.002%	3.1937	0.001%	3.1937	0.000%	3.1937	0.000%	3.1937	0.000%
0.06	3.0776	3.0776	0.001%	3.0776	0.001%	3.0776	0.000%	3.0776	0.000%	3.0776	0.000%
0.08	2.9161	2.9161	0.001%	2.9161	0.000%	2.9161	0.000%	2.9161	0.000%	2.9161	0.000%
0.1	2.7409	2.7409	0.001%	2.7409	0.000%	2.7409	0.000%	2.7409	0.000%	2.7409	0.000%

β = 0.1	Adopted (25592)	Mesh #1 (398)		Mesh #2 (526)		Mesh #3 (934)		Mesh #4 (1922)		Mesh #5 (2744)	
Kn	Nu	Nu	ε_r	Nu	ε_r	Nu	ε_r	Nu	ε_r	Nu	ε_r
0	0.6153	0.6155	0.035%	0.6154	0.011%	0.6153	0.003%	0.6153	0.001%	0.6153	0.000%
0.02	0.6742	0.6743	0.022%	0.6742	0.007%	0.6742	0.002%	0.6742	0.000%	0.6742	0.000%
0.04	0.7055	0.7056	0.014%	0.7055	0.005%	0.7055	0.001%	0.7055	0.000%	0.7055	0.000%
0.06	0.7211	0.7211	0.010%	0.7211	0.003%	0.7211	0.001%	0.7211	0.000%	0.7211	0.000%
0.08	0.7272	0.7272	0.007%	0.7272	0.002%	0.7272	0.001%	0.7272	0.000%	0.7272	0.000%
0.1	0.7274	0.7274	0.005%	0.7274	0.002%	0.7274	0.000%	0.7274	0.000%	0.7274	0.000%

Table 2.

		β=0.1		β=0.5		β=1	
		Case B	Case C	Case B	Case C	Case B	Case C
Maximum discrepancy on Nu	*Br=0.1*	23.23%	24.69%	11.01%	33.77%	11.55%	38.28%
	Br=-0.1	-21.28%	-19.04%	-10.93%	-28.87%	-11.78%	-32.44%
Maximum discrepancy on Nu_{sw}	*Br=0.1*	22.91%	24.38%	10.94%	33.75%	11.49%	38.26%
	Br=-0.1	-21.68%	-19.44%	-10.95%	-28.88%	-11.80%	-32.45%

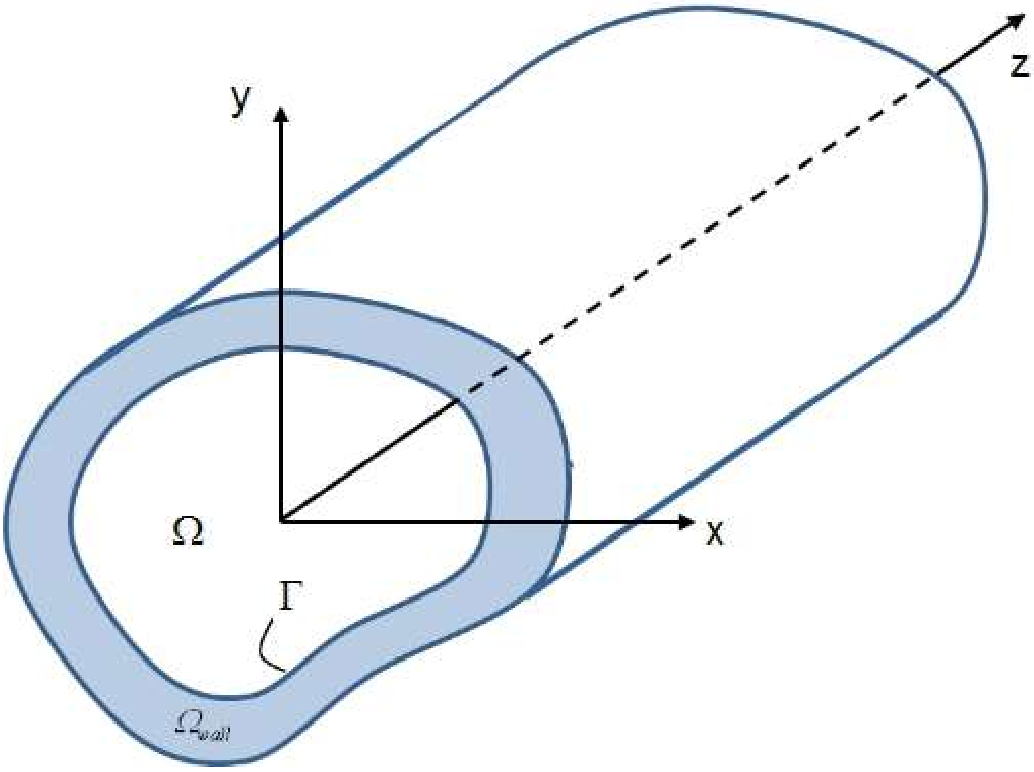

y
z
x
Ω
Γ
Ω_{wall}

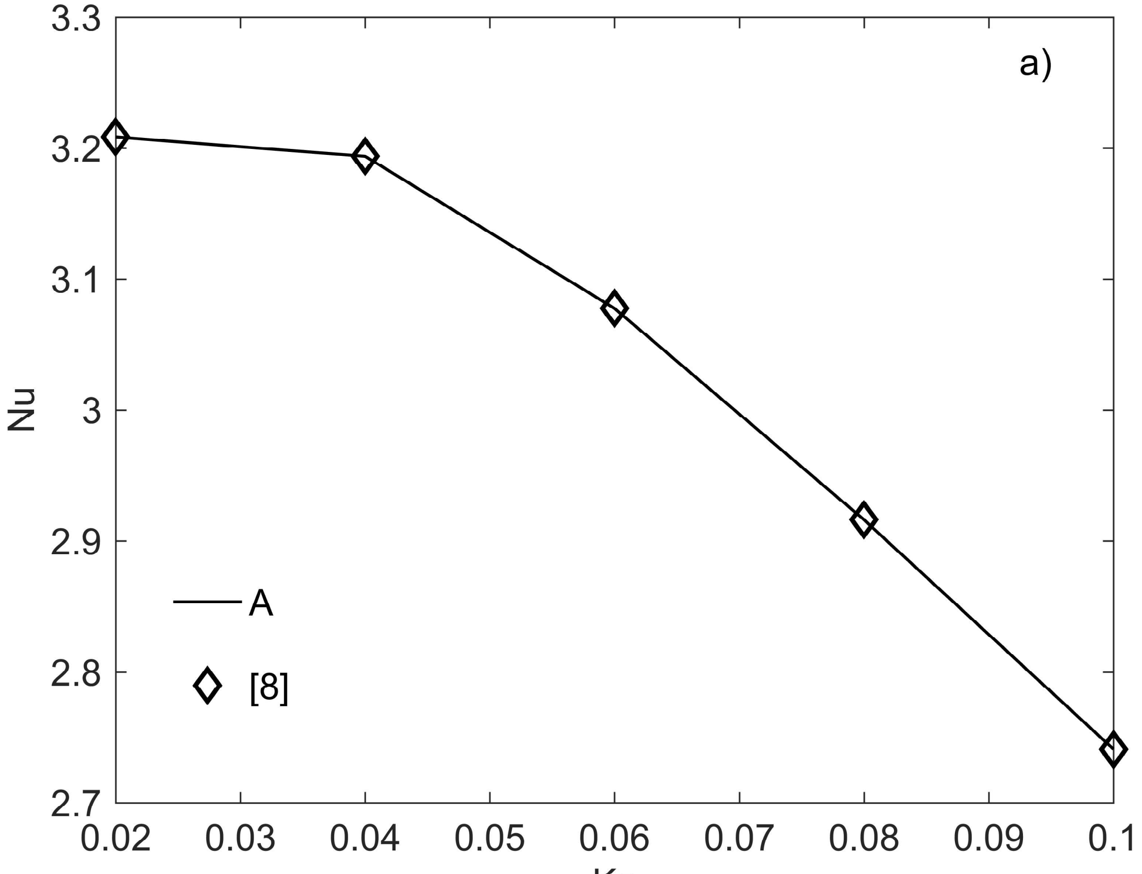

a)
Nu
Kn
A
[8]
3.3
3.2
3.1
3
2.9
2.8
2.7
0.02
0.03
0.04
0.05
0.06
0.07
0.08
0.09
0.1

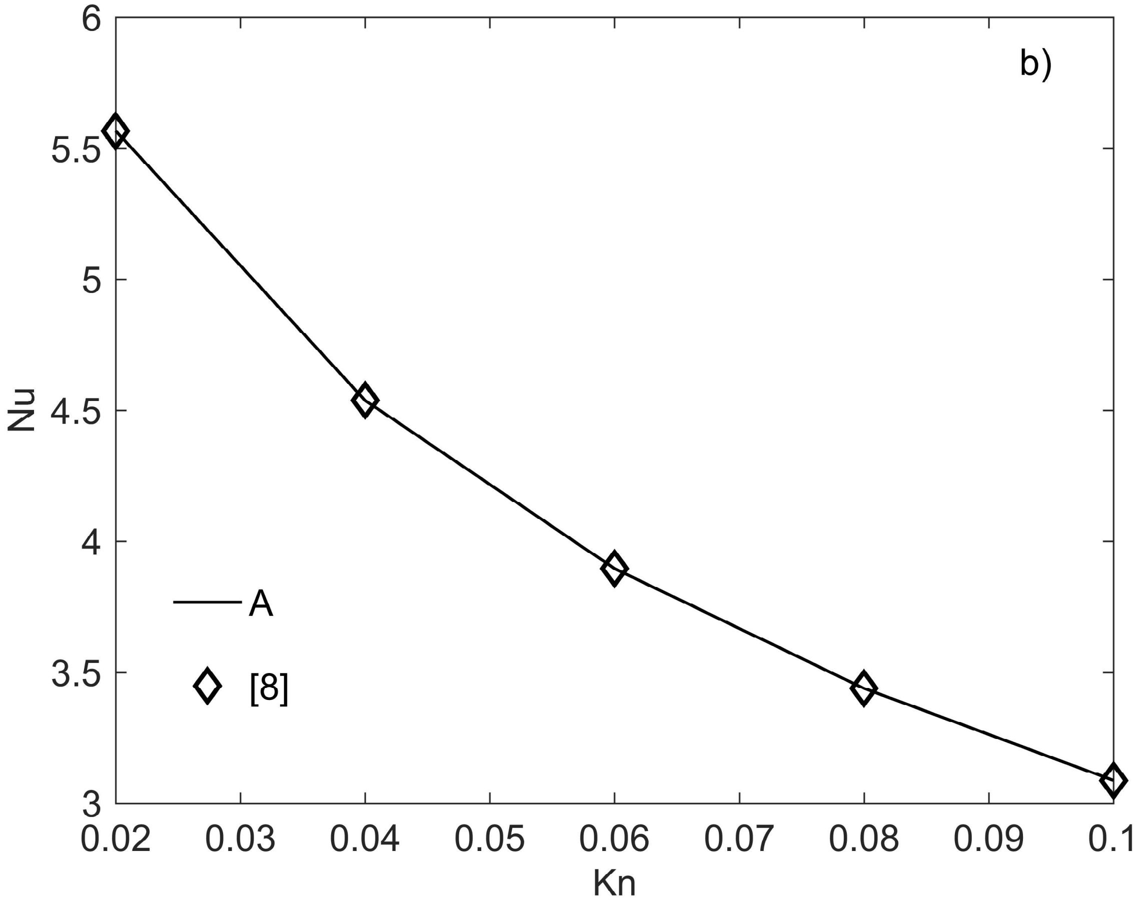

b)
Nu
Kn
A
[8]
6
5.5
5
4.5
4
3.5
3
0.02
0.03
0.04
0.05
0.06
0.07
0.08
0.09
0.1

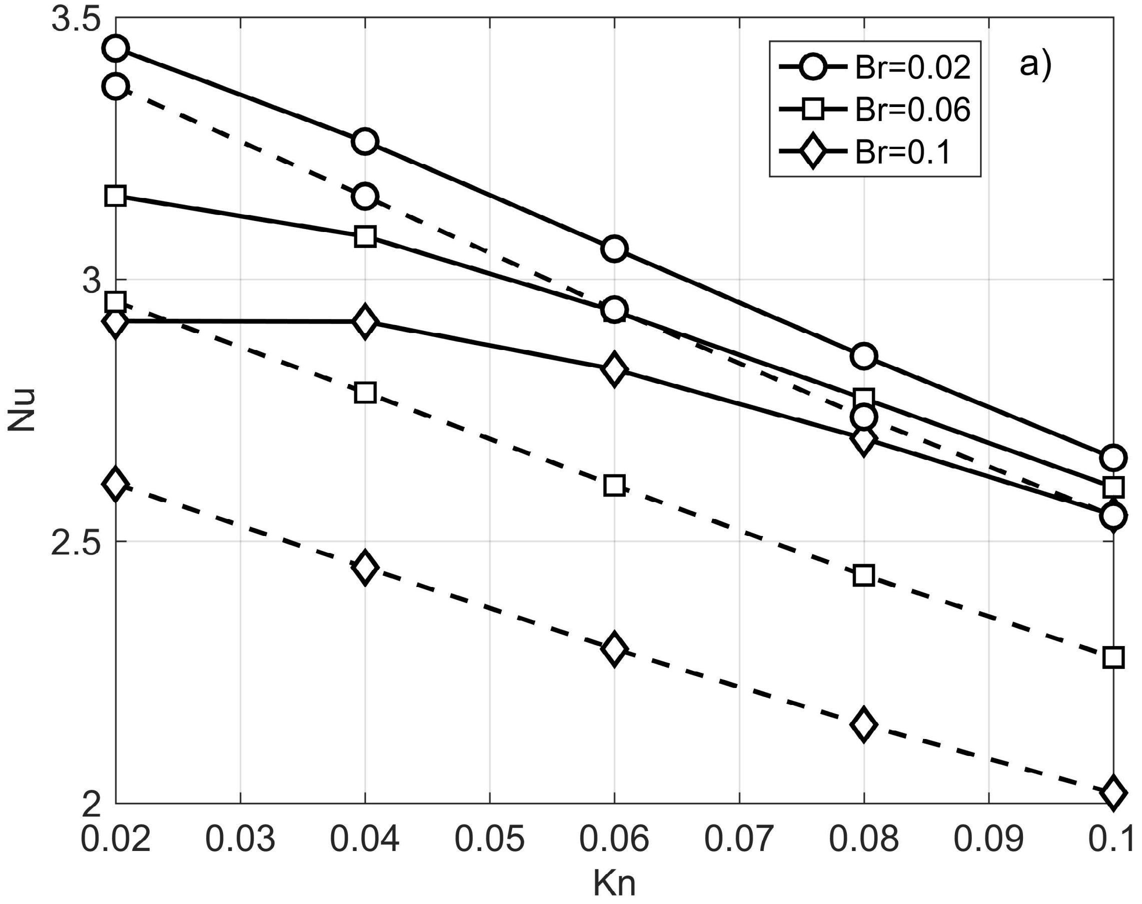

Br=0.02
Br=0.06
Br=0.1
a)
Nu
Kn
3.5
3
2.5
2
0.02
0.03
0.04
0.05
0.06
0.07
0.08
0.09
0.1

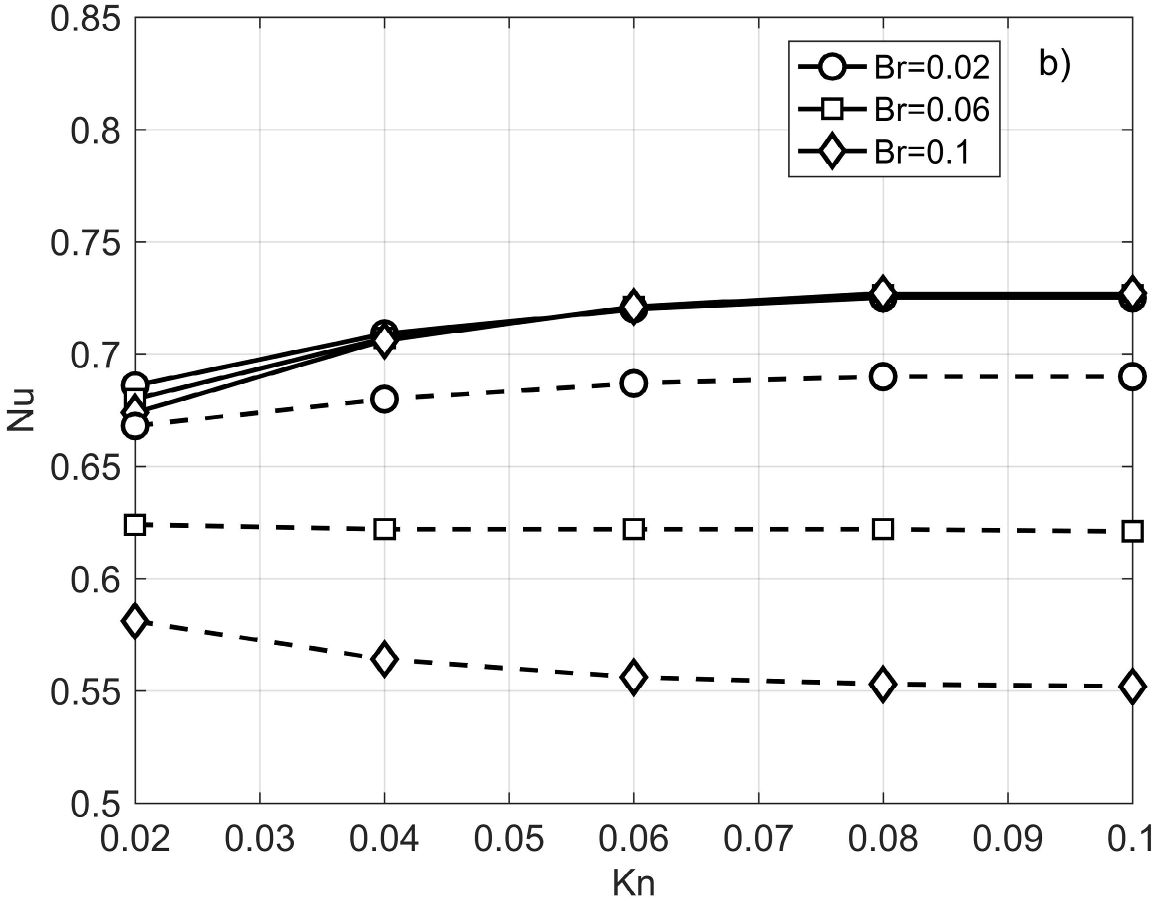

0.85
0.8
0.75
0.7
0.65
0.6
0.55
0.5
Nu
0.02
0.03
0.04
0.05
0.06
0.07
0.08
0.09
0.1
Kn
Br=0.02
Br=0.06
Br=0.1
b)

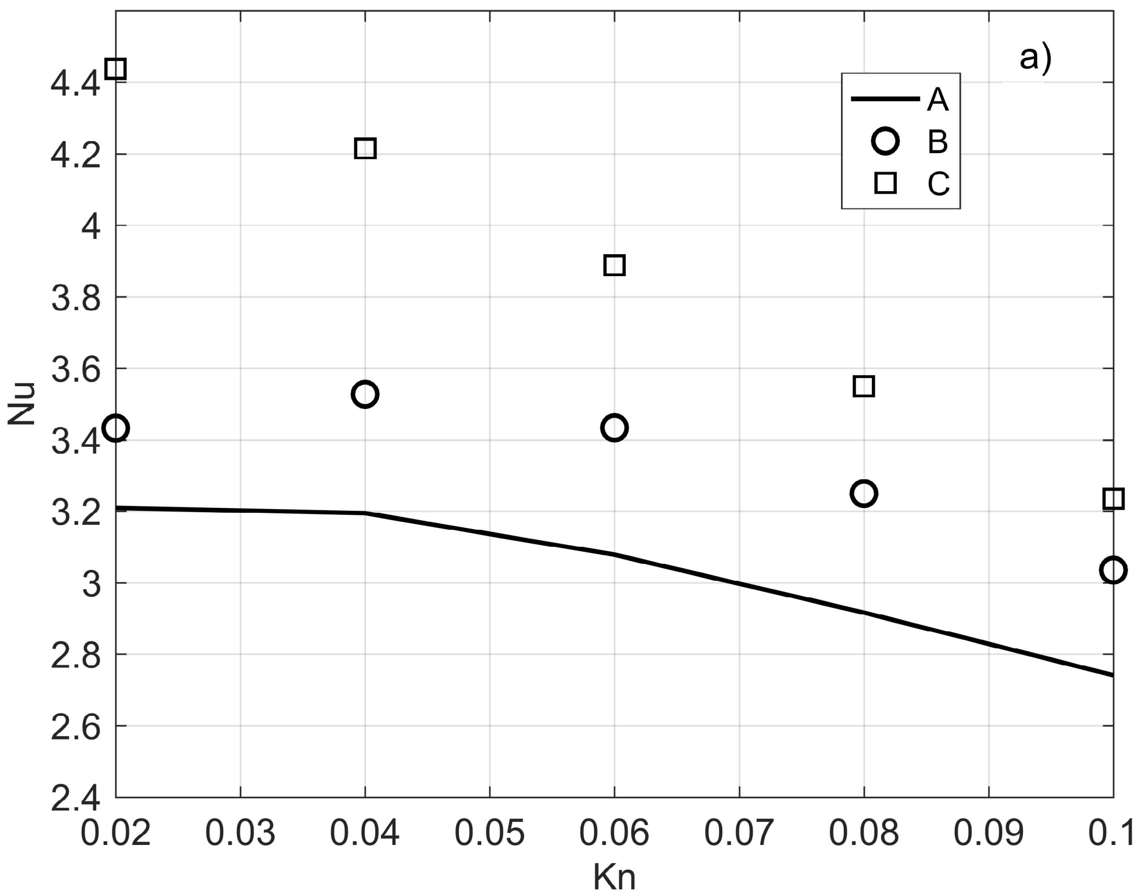
a)
A
B
C
Nu
Kn
4.4
4.2
4
3.8
3.6
3.4
3.2
3
2.8
2.6
2.4
0.02
0.03
0.04
0.05
0.06
0.07
0.08
0.09
0.1

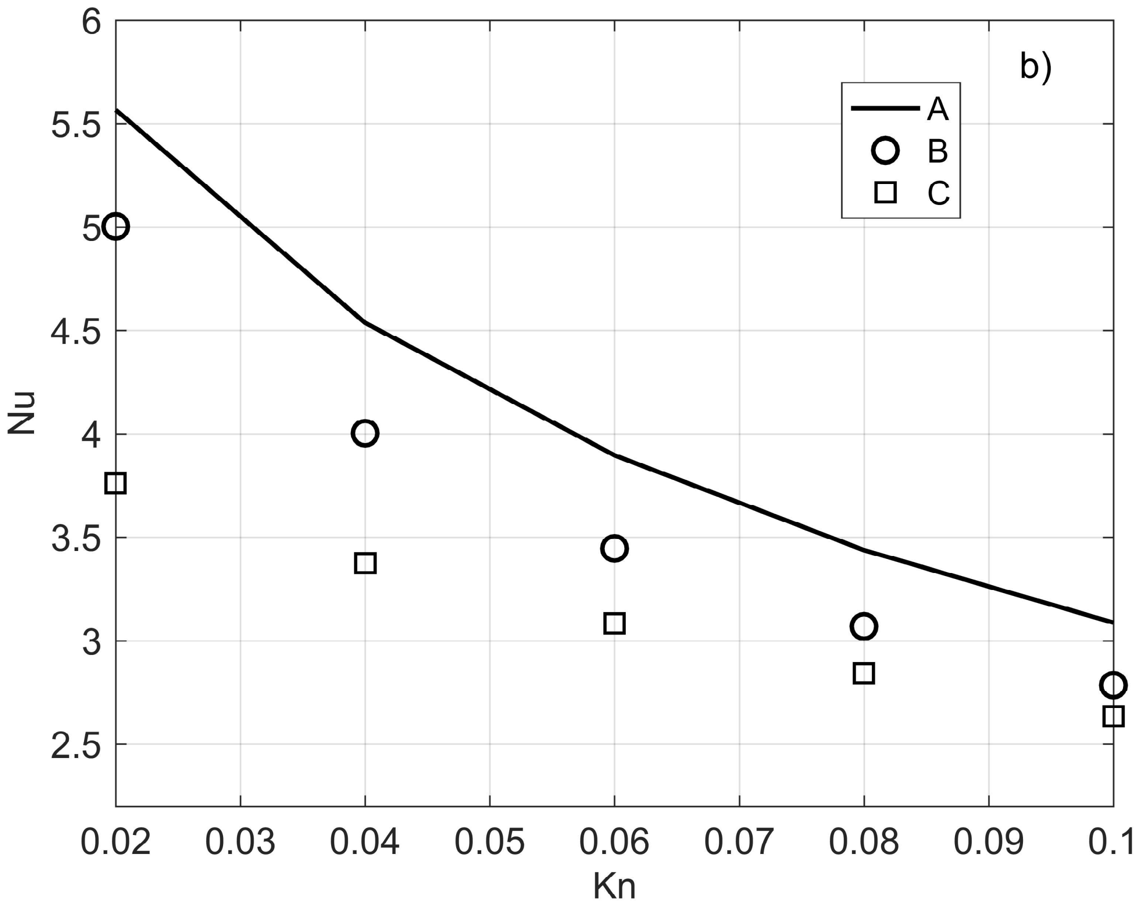
b)
A
B
C
Nu
Kn
6
5.5
5
4.5
4
3.5
3
2.5
0.02
0.03
0.04
0.05
0.06
0.07
0.08
0.09
0.1

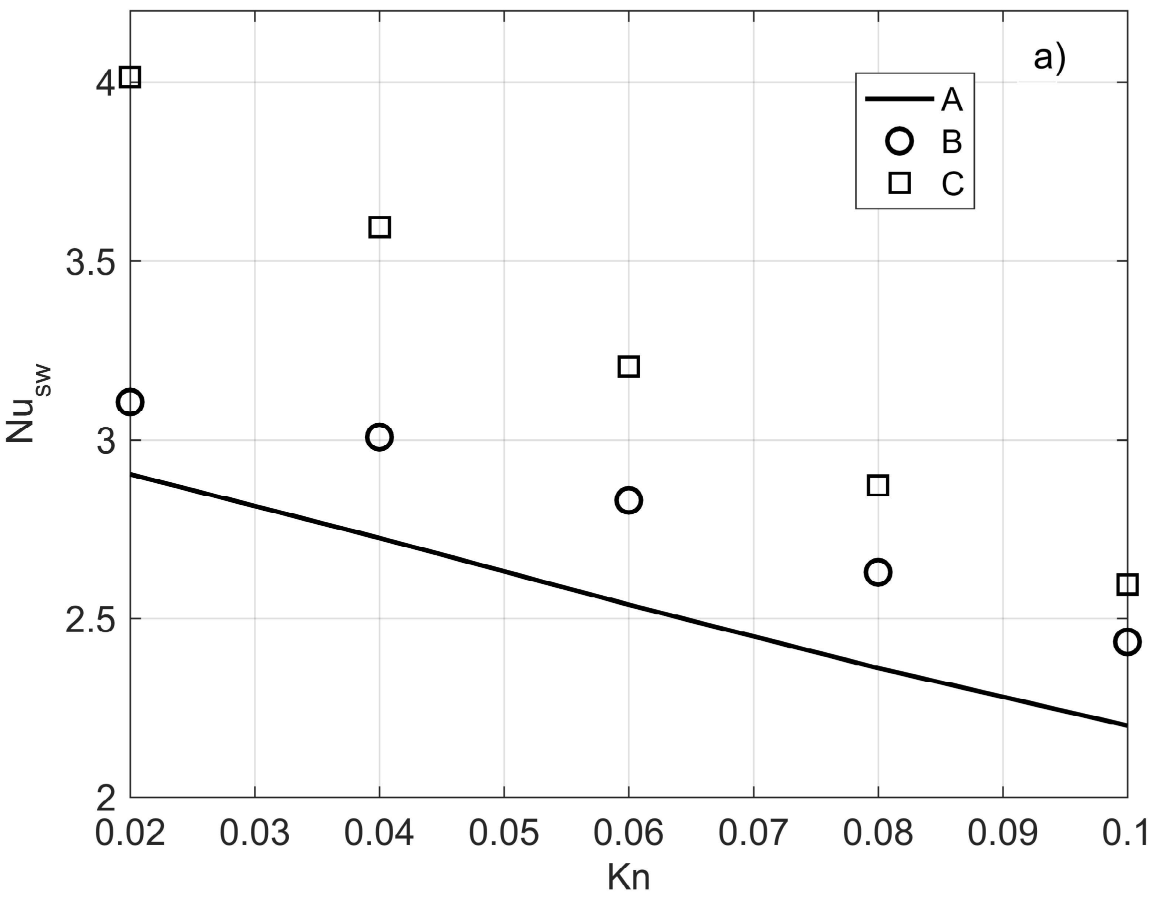

a)
A
B
C
Nu_{sw}
Kn
4
3.5
3
2.5
2
0.02
0.03
0.04
0.05
0.06
0.07
0.08
0.09
0.1

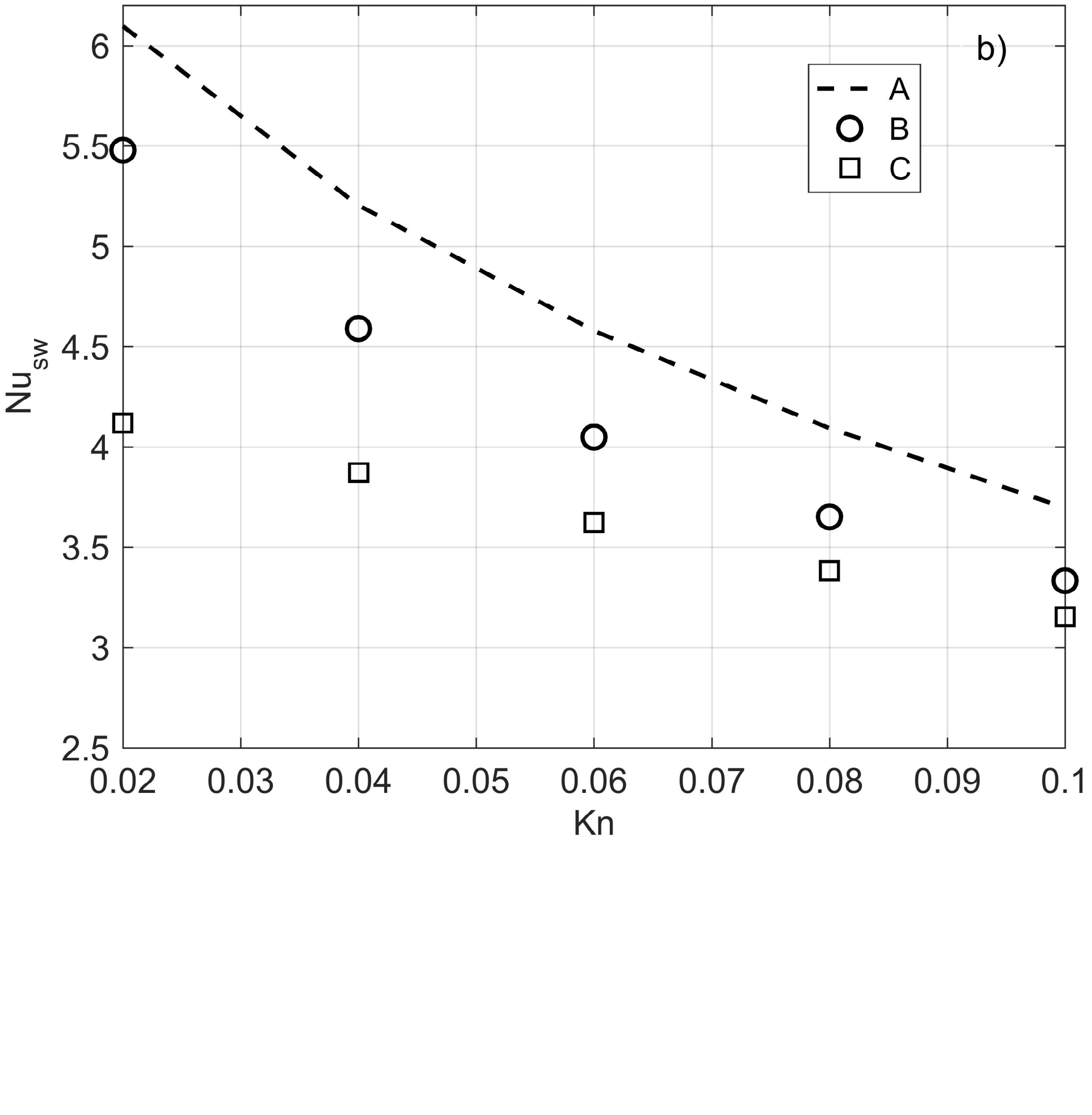

b)
A
B
C
6
5.5
5
4.5
4
3.5
3
2.5
Nu_{sw}
0.02
0.03
0.04
0.05
0.06
0.07
0.08
0.09
0.1
Kn

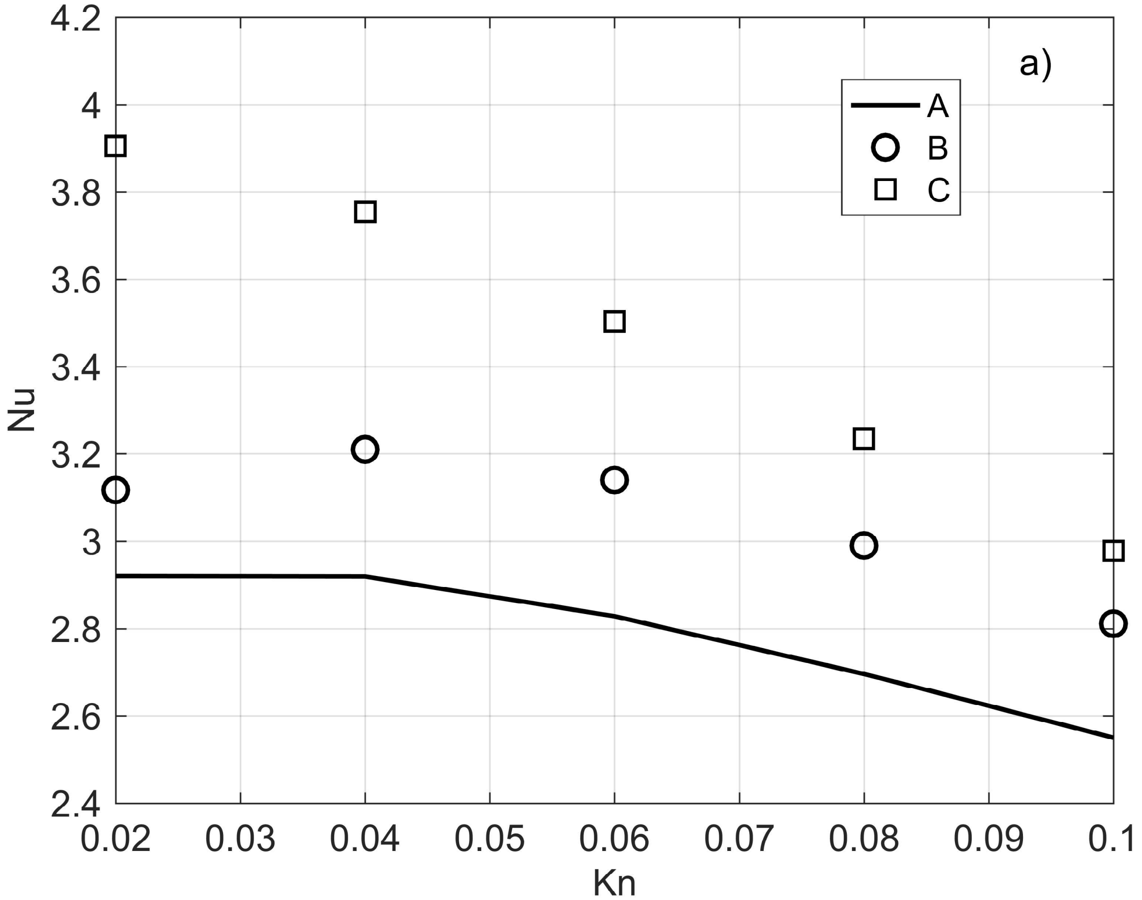

a)
A
B
C
Nu
Kn
4.2
4
3.8
3.6
3.4
3.2
3
2.8
2.6
2.4
0.02
0.03
0.04
0.05
0.06
0.07
0.08
0.09
0.1

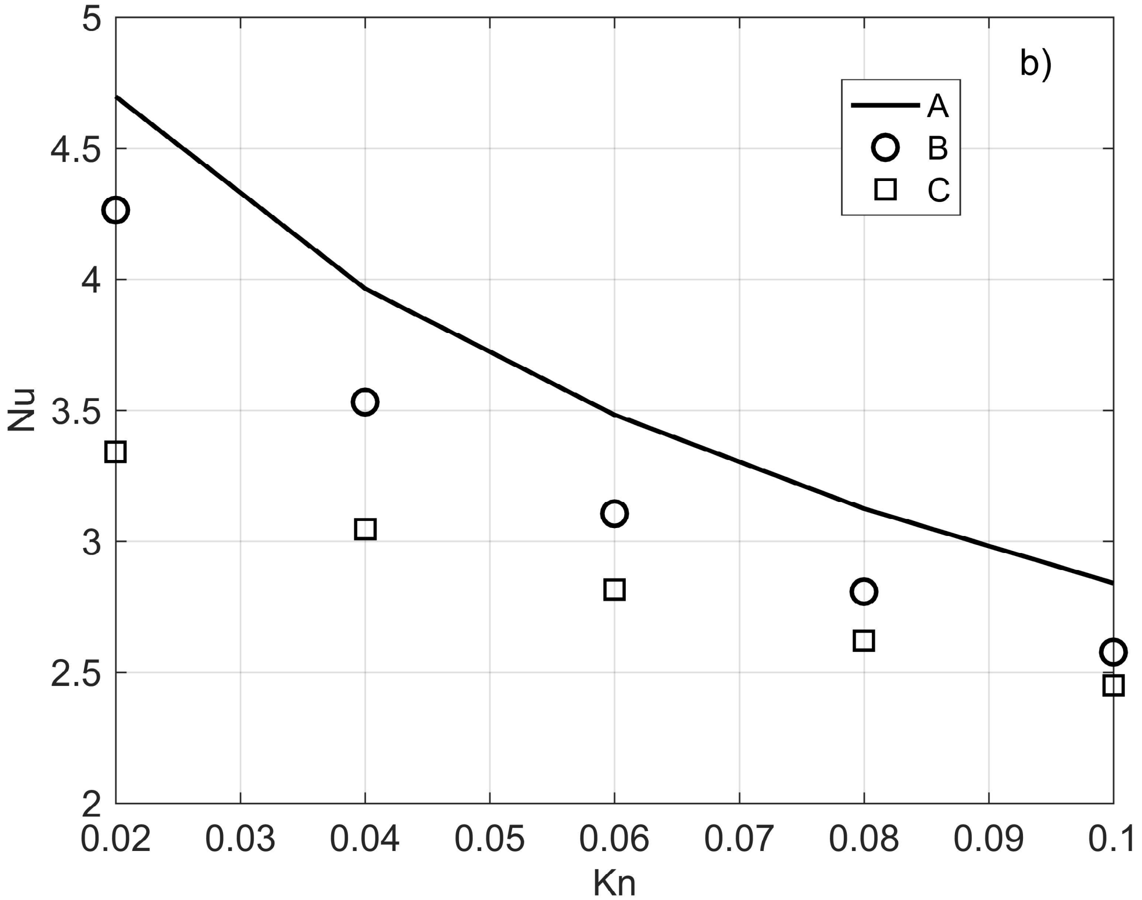

b)
A
B
C
Nu
Kn
5
4.5
4
3.5
3
2.5
2
0.02
0.03
0.04
0.05
0.06
0.07
0.08
0.09
0.1

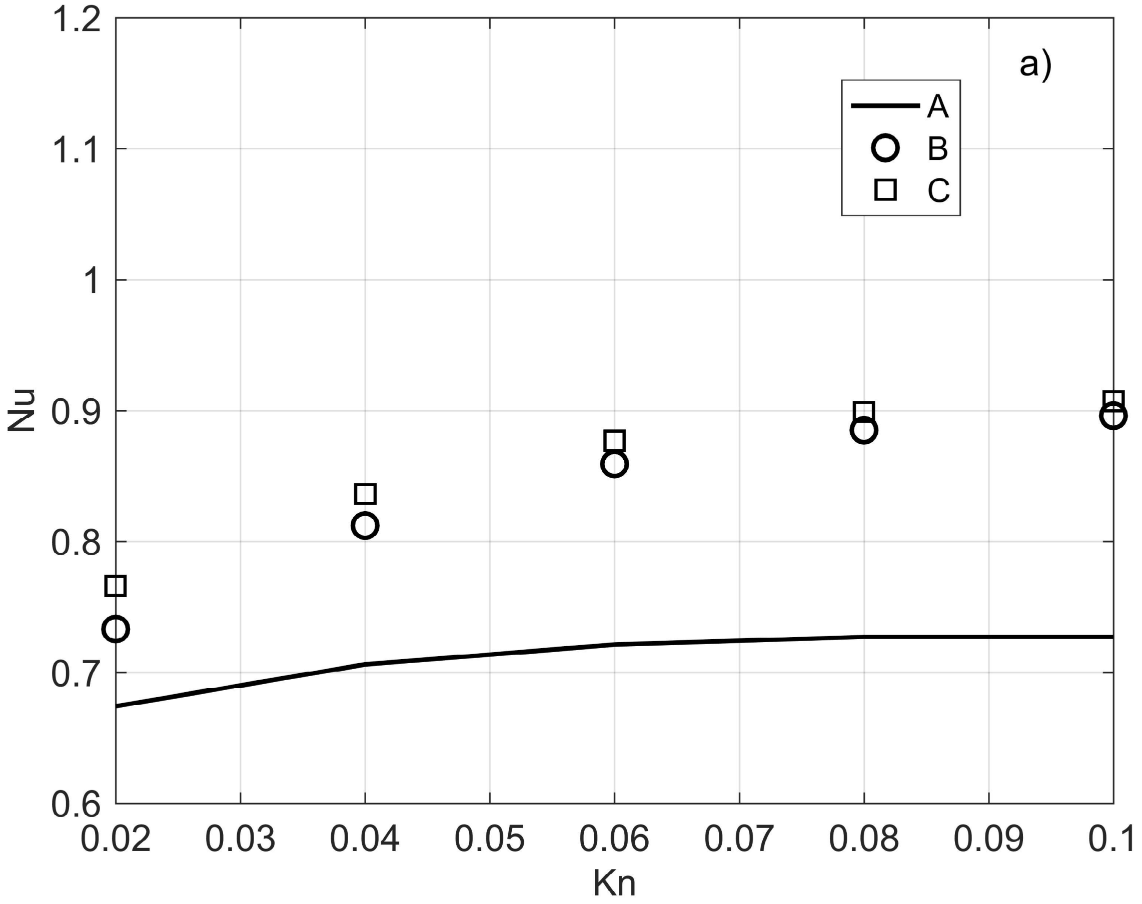

a)
A
B
C
Nu
Kn
1.2
1.1
1
0.9
0.8
0.7
0.6
0.02
0.03
0.04
0.05
0.06
0.07
0.08
0.09
0.1

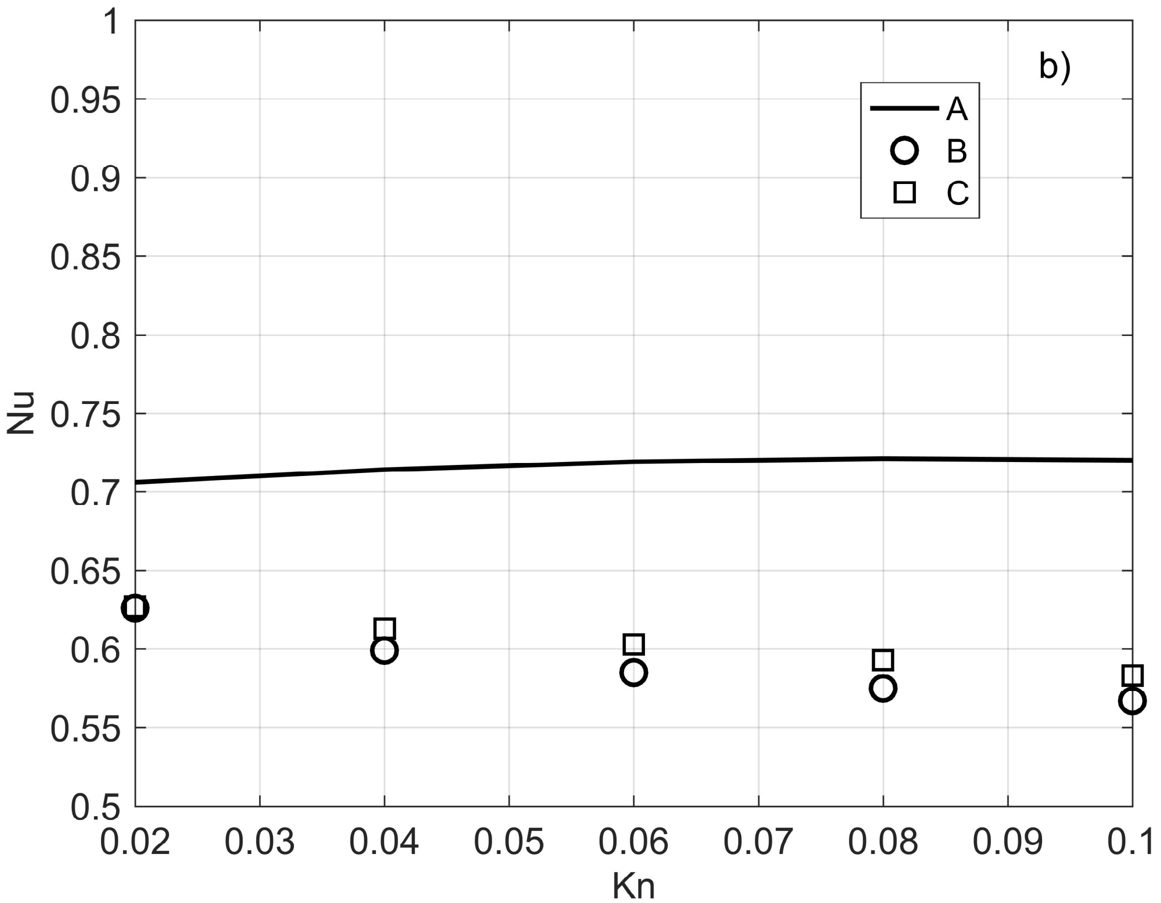

b)
A
B
C
Nu
Kn
1
0.95
0.9
0.85
0.8
0.75
0.7
0.65
0.6
0.55
0.5
0.02
0.03
0.04
0.05
0.06
0.07
0.08
0.09
0.1